A Statistical Closure of a Low-Order Barotropic Model

FRANK M. SELTEN

Royal Netherlands Meteorological Institute, De Bilt, the Netherlands

(Manuscript received 28 April 1995, in final form 16 July 1996)

ABSTRACT

In this paper, an attempt to close a low-order barotropic model for the neglected interactions in a perfect model setting is described. A barotropic T21 model with forcing and dissipation included is reformulated in terms of its EOFs. The EOFs are calculated from a long integration, and evolution equations are derived for the EOF amplitudes. A low-order EOF model is obtained by retaining only the 20 most dominant EOF structures and neglecting interactions with the remaining 211 EOFs. An attempt is made to describe the tendency error of the EOF model with a linear combination of resolved EOF amplitudes plus their quadratic combinations. The linear combination minimizes in a least squares sense the tendency error of the EOF model on the attractor of the full T21 model. It is found that, only if quadratic combinations of EOF amplitudes are taken into account, the closure reduces the tendency error substantially. The impact of the closure on the forecast skill of the EOF model is studied by making 100 3-week forecasts starting from independent initial conditions on the attractor of T21. The average useful forecast range increases from 12 days without closure to 18 days with closure. However, the method seems questionable in two aspects. First, the corrections to the coefficients of the evolution equations of the EOF amplitudes are as large as the coefficients themselves. Second, the closed EOF model could not simulate the climate. The closed model does not conserve energy in the absence of forcing and dissipation, and for this reason does not possess a stable attractor. Modifications to the proposed closure are mentioned to solve this problem. In conclusion, the proposed closure without the mentioned modifications leads to a statistical model that has an improved predictive skill but fails to simulate the climate of the original T21 barotropic model.

1. Introduction

In numerical models of the atmosphere, the continuous atmosphere is described at a finite resolution. The effect of neglected small-scale flow structures needs to be parameterized in terms of the resolved part of the flow. One usually refers to this problem as the closure problem. Most numerical models parameterize the neglected interactions with a diffusion term. Often the strength of the viscosity is tuned in order to reproduce the observed kinetic energy spectrum. Other tuning criteria were formulated by MacVean (1983) by investigating the effect of dissipation on the development of baroclinic waves in a baroclinic, spectral model. Although the effect of the nonresolved scales appears partly dissipative, it has also been recognized that small scales often reinforce larger-scale flow structures or have effects on the larger scales that cannot be described by diffusion terms. The maintenance of blocking structures by synoptic-scale transient eddies is a well-known example (e.g., Ilari and Marshall 1983). Another approach to the closure problem was proposed by Leith (1978). He described a general method to empirically correct an atmospheric model. It is based on the minimization of the difference between observed and model-generated tendencies by linear regression. Faller and Schemm (1977) applied this method to the problem of parameterizing the effects of unresolved scales of motion in a simple two-dimensional advection model with forcing and dissipation on a rectangular grid. The statistical correction terms improved the predictive skill of the coarse-grid model substantially, but extended integrations turned out to be unstable. In the present paper, this method is evaluated in a model that is more relevant to atmospheric dynamics. A barotropic spectral T21 model with forcing and dissipation terms included is used in a perfect model approach. The model circulation evolves around a realistic mean circulation. The model is reformulated in terms of its EOFs and truncated to the leading 20 EOFs. The model error in the EOF model is entirely due to neglecting interactions with the unresolved part of the flow. An attempt is made to parameterize these interactions taking Leith's approach. The method is described in section 2 in the context of the EOF model. In section 3, experiments are described and the results are presented and discussed. Some concluding remarks are given in section 4.

Corresponding author address: Frank M. Selten, Royal Netherlands Meteorological Institute, P.O. Box 201, 3730 AE De Bilt, the Netherlands.
E-mail: selten@knmi.nl

2. Outline of the method

Suppose we have a deterministic atmospheric model with N variables, which can be written in the form

$$\dot{\psi}_i(t) = \alpha'_i + \sum_{j=1}^{N} \beta'_{ij}\psi_j(t) + \sum_{j=1}^{N}\sum_{k=j}^{N} \gamma'_{ijk}\psi_j(t)\psi_k(t) \quad \text{for } i = 1, \ldots, N. \tag{1}$$

The spectral method, such as that of Machenhauer (1991), applied to the barotropic vorticity equation leads to evolution equations of this form. The variables ψ_i then correspond to the spectral expansion coefficients of the streamfunction. These equations can be integrated numerically. If the attractor of the system of equations has a dimension much smaller than the number of variables N, or if the dynamics is dominated by interactions among a small number of dominant flow structures, we may try to simulate the dynamics with a reduced number of variables. The way in which we have tried to achieve this (Selten 1993, 1995) is first to calculate empirical orthogonal functions from the dataset and second to derive evolution equations for the amplitudes of the EOFs from Eq. (1). The EOFs are ordered according to the amount of energy projected onto it. Since only a small fraction of the total energy is projected onto the subspace spanned by the trailing EOFs, we hypothesize that their influence on the time evolution of the dominant EOFs is small. The evolution equations for the amplitudes of the EOFs are given by

$$\dot{a}_i(t) = \alpha_i + \sum_{j=1}^{T} \beta_{ij}a_j(t) + \sum_{j=1}^{T}\sum_{k=j}^{T} \gamma_{ijk}a_j(t)a_k(t) + \epsilon_i^T(t), \quad \text{for } i = 1, \ldots, T. \tag{2}$$

The error ϵ_i^T introduced in the time derivative of a_i by retaining only the first T EOFs ($T \ll N$) is given by

$$\epsilon_i^T(t) = \sum_{j=T+1}^{N} \beta_{ij}a_j(t) + \sum_{j=T+1}^{N}\sum_{k=j}^{N} \gamma_{ijk}a_j(t)a_k(t) + \sum_{j=1}^{T}\sum_{k=T+1}^{N} \gamma_{ijk}a_j(t)a_k(t), \quad \text{for } i = 1, \ldots, T, \tag{3}$$

where the first double sum contains the interactions among unresolved components and the second one contains interactions between the resolved and unresolved components. The subject of this study is to account for this small tendency error.

We propose to minimize the mean-squared value of the tendency error by adjusting the coefficients in the evolution of Eq. (2). The adjusted evolution equations are given by

$$\tilde{a}_i(t) = \alpha_i + \delta\alpha_i + \sum_{j=1}^{T} (\beta_{ij} + \delta\beta_{ij})a_j(t) + \sum_{j=1}^{T}\sum_{k=j}^{T} (\gamma_{ijk} + \delta\gamma_{ijk})a_j(t)a_k(t), \quad \text{for } i = 1, \ldots, T, \tag{4}$$

and the optimal variations $\delta\alpha_i$, $\delta\beta_{ij}$, and $\delta\gamma_{ijk}$ are determined by the minimization of the functional

$$F_i(\delta\alpha_i, \delta\beta_{ij}, \delta\gamma_{ijk}) = \overline{[\dot{a}_i - \tilde{a}_i]^2} \quad \text{for } i = 1, \ldots, T. \tag{5}$$

The overbar denotes a time average. Substitution of Eqs. (2) and (4) into Eq. (5) gives

$$F_i(\delta\alpha_i, \delta\beta_{ij}, \delta\gamma_{ijk}) = \overline{\left[\epsilon_i^T(t) - \delta\alpha_i - \sum_{j=1}^{T} \delta\beta_{ij}a_j(t) - \sum_{j=1}^{T}\sum_{k=j}^{T} \delta\gamma_{ijk}a_j(t)a_k(t)\right]^2}, \quad \text{for } i = 1, \ldots, T. \tag{6}$$

This equation can be interpreted as follows: we look for a linear combination of the amplitudes and quadratic combinations of the amplitudes of the retained EOFs, which, in a least squares sense, best describes the tendency error.

If we now introduce new variables b_j that are equal to the resolved EOF amplitudes and all possible quadratic combinations of the EOF amplitudes according to

$$b_j = a_j, \quad \text{for} \quad j = 1, \ldots, T$$
$$b_l = a_j \cdot a_k, \quad \text{for} \begin{cases} j = 1, \ldots, T \\ k = j, \ldots, T \\ l = k + (T - 0.5j)(j - 1) + T, \end{cases} \tag{7}$$

the functional F_i takes a more concise form:

$$F_i(\delta\alpha_i, \delta c_{ij}) = \overline{\left[\epsilon_i^T(t) - \delta\alpha_i - \sum_{j=1}^{0.5T(T+3)} \delta c_{ij}b_j(t)\right]^2}, \quad \text{for } i = 1, \ldots, T, \tag{8}$$

where δc_{ij} is a different notation for the variations $\delta\beta_{ij}$ and $\delta\gamma_{ijk}$ according to

$$\delta c_{ij} = \delta\beta_{ij}, \quad \text{for} \quad i, j = 1, \ldots, T$$
$$\delta c_{il} = \delta\gamma_{ijk}, \quad \text{for} \begin{cases} i, j = 1, \ldots, T \\ k = j, \ldots, T \\ l = k + (T - 0.5j)(j - 1) + T. \end{cases} \tag{9}$$

An additional demand is that the mean tendency error of the closed model should vanish. This demand is not really necessary, but it ensures that the closed model will not experience a large initial drift on average. This gives a relationship between the variations $\delta\alpha_i$ and δc_{ij}:

$$\overline{\epsilon_i^T(t)} - \delta\alpha_i - \sum_{j=1}^{0.5T(T+3)} \delta c_{ij}\overline{b_j(t)} = 0, \quad \text{for } i = 1, \ldots, T. \tag{10}$$

Substitution of this relationship into Eq. (8) gives

$$F_i(\delta c_{ij}) = \overline{\left\{\epsilon_i^T(t) - \overline{\epsilon_i^T(t)} - \sum_{j=1}^{0.5T(T+3)} \delta c_{ij}[b_j(t) - \overline{b_j(t)}]\right\}^2}, \quad \text{for } i = 1, \ldots, T. \tag{11}$$

The extrema of F_i are easily determined by putting the partial derivatives with respect to δc_{ik} to zero:

$$\frac{\partial F_i}{\partial \delta c_{ik}} = \overline{2\left\{\epsilon_i^T(t) - \overline{\epsilon_i^T(t)} - \sum_{j=1}^{0.5T(T+3)} \delta c_{ij}[b_j(t) - \overline{b_j(t)}]\right\}[b_k(t) - \overline{b_k(t)}]}$$

$$= 0 \qquad \text{for} \begin{cases} i = 1, \ldots, T \\ k = 1, \ldots, 0.5T(T+3). \end{cases} \tag{12}$$

Rewriting this equation and using

$$\text{cov}(x, y) \equiv \overline{[x(t) - \overline{x(t)}]\,[y(t) - \overline{y(t)}]}$$

gives

$$\sum_{j=1}^{0.5T(T+3)} \text{cov}(b_j, b_k)\delta c_{ij} = \text{cov}(\epsilon_i^T, b_k), \quad \text{for} \begin{cases} i = 1, \ldots, T \\ k = 1, \ldots, 0.5T(T+3). \end{cases} \tag{13}$$

This linear system can be solved for the optimal variations δc_{ij} that minimize the tendency error in a least squares sense. This expression is similar to Eq. (7.8) in Leith (1978), except that in this case the variables b_j also contain quadratic combinations of the prognostic model variables. Leith considered corrections to the constant and linear model terms only.

In textbooks on statistical analysis, Eq. (13) is often referred to as the normal equation. One has to be aware of the fact that this linear system is likely to be an ill-posed problem. The best way to deal with this is to follow the procedure using singular value decomposition as described in Press et al. (1986). For clarity, we will apply this procedure in the terminology of EOF analysis. To facilitate the solution of Eq. (13), an EOF analysis is performed on the time series of the variables b_j and the problem is formulated in terms of these EOFs. We will refer to these EOFs as bEOFs to prevent confusion with the EOFs in which the model is formulated. The result is that the covariance matrix in (13) is diagonalized and the linear system of Eq. (13) decouples and becomes trivial to solve. Denoting the matrix with the bEOFs as columns by J and the corresponding amplitudes by g, Eq. (13) becomes, after some manipulation,

$$\delta c_{ij} = \sum_{k=1}^{0.5T(T+3)} \frac{\text{sd}(\epsilon_i^T)}{\text{sd}(g_k)}\text{cor}(\epsilon_i^T, g_k)J_{jk}, \qquad \text{for} \begin{cases} i = 1, \ldots, T \\ j = 1, \ldots, 0.5T(T+3), \end{cases} \tag{14}$$

where sd(.) denotes the standard deviation and cor(.,.) the correlation coefficient. The corrections δc_{ij} are given by a sum over the bEOFs. From this expression it becomes clear that small sampling errors in the estimated correlation between the tendency error and the bEOF amplitudes will be magnified in case of bEOFs with small eigenvalues, that is, small variances. For bEOFs with eigenvalues orders of magnitude smaller than the variance of the tendency error, the solution becomes close to singular. Including these bEOFs in the regression causes the estimated corrections to become large and sensitive to small changes in the estimates of the correlations and variances. If the estimates turn out to be sample dependent, one could decide to exclude the bEOFs with eigenvalues orders of magnitude smaller than the variance of the tendency error from the regression. This would then still allow a robust estimation of the corrections δc_{ij}.

A simplification is possible if we restrict the procedure to linear combinations of EOF amplitudes, in other words, if we do not vary the interaction coefficients γ_{ijk}. In that case, the covariance matrix in (13) is diagonal since the EOF amplitudes are uncorrelated in time. Thus the linear system of Eqs. (13) decouples and reduces to

$$\delta\beta_{ik} = \frac{\mathrm{sd}(\epsilon_i^T)}{\mathrm{sd}(a_k)}\mathrm{cor}(\epsilon_i^T, a_k), \quad \text{for } i, k = 1, \ldots, T. \quad (15)$$

This result is intuitively clear. The correlation measures to what extent two time series are linearly dependent. If the correlation between the time series of the tendency error and the time series of a particular EOF amplitude is large, it implies that part of the tendency error can be described by including the time series of this EOF in the linear combination.

One final remark. It is relevant to note that it is not required that we know the coefficients of the truncated EOF model a priori. Instead we could start from an EOF model with all coefficients in Eq. (2) equal to zero, in which case the tendency error is equal to the true tendency and we would find the same optimal model. Viewed this way, our approach is similar to that of Hasselman (1988), which described a very general statistical method to reduce complex dynamical systems. In his approach, not only are the coefficients of the evolution equations varied in order to minimize the tendency error, but so are the base patterns used in the expansion of the flow field (referred to as ''principal interaction patterns,'' hereafter PIP). Achatz (1995) applied this method in the context of a quasigeostrophic two-layer model; Kwasniok (1996) determined PIPs of the same barotropic model that is used in this paper.

3. Experiments and results

a. Model and data

We tested the above-described closure procedure on the EOF version of the barotropic spectral model described in Selten (1995, hereafter SE). For this model $N = 231$. In SE, EOFs were calculated from a 50 000-day integration of the barotropic model. Evolution equations were derived for the EOF amplitudes. In the present study these evolution equations will be modified empirically to reduce the tendency error of a 20-component EOF model, denoted by EOF[20], in which the interactions with the remaining 211 EOFs are neglected. Three independent datasets will be used. These were produced by an extended integration with the barotropic model using a fourth-order Runge–Kutta time stepping scheme with a time step of 8 h. Two datasets each cover a 250 000-day period with the model state archived every fifth day. These two datasets will be used to determine the empirical corrections to the EOF model. The third dataset covers a 10 000-day period with the model state archived once a day. This dataset will be used to evaluate the predictive skill of a low-order EOF model with and without empirical corrections.

The tendency error ϵ_i^T (where i refers to the index of the EOF and T to the truncation limit) was calculated at every archived state on the attractor of the barotropic model in one of the 250 000-day datasets for truncations at 10, 20, 30, 40, 60, and 80 EOFs. In order to evaluate the tendency error, we calculated the variance of the tendency error of each EOF, normalized by the variance of the tendency of that EOF. The results are plotted in Fig. 1a for the first 20 EOFs. It is clear that the tendency error variance rapidly decreases as more EOFs are retained. At a truncation of 10 EOFs, the tendency error is rather large. For EOF 3, the error variance is almost as large as the variance of the tendency itself. At a truncation of 20, the error variance is reduced by more than half the error variance at truncation 10. At a truncation of 80, the error variance is only a few percent of the variance of the tendency for the first 20 EOFs. We also calculated the correlation between the time series of the true and approximated EOF tendencies in the truncated EOF model. These results are plotted in Fig. 1b. The correlations are poor at a truncation of 10 EOFs, much better at a truncation of 20 EOFs, and close to one for the first 20 EOFs at a truncation of 80. Both figures indicate, that among the dominant EOFs, EOF 3 has strongest interactions with the neglected components. These results show that at a truncation of 80 EOFs the tendencies of the dominant EOFs are close to the true tendencies. With less than 80 EOFs, the tendency error rapidly increases.

b. Linear correction

We tried to reduce the tendency error at truncation 20 by adjusting the coefficients in the evolution equations of the EOF amplitudes according to the method described above. First we tried to describe the tendency error by a linear combination of the retained EOF amplitudes. Unfortunately, Eq. (15) is not applicable in this case, since the EOFs in SE were not calculated from anomalies but from the total model state. The covariance matrix is thus not diagonalized by these EOFs. Instead, we solved Eq. (13) restricted to corrections to the linear terms only (δc_{ij} is zero for $j > T$). It means that the size of the problem is reduced from $0.5\ T\ (T + 3)$ to T. The corrections are calculated twice using the two independent 250 000-day datasets. Comparing both sets of coefficients gives an indication of the sampling error. The bEOFs, the standard deviation of the bEOFs, the standard deviation of the tendency error, and the correlations between the bEOFs and the tendency error were estimated and substituted in Eqs. (14) to obtain the corrections $\delta\beta_{ij}$. The corrections to the constant terms $\delta\alpha_i$ were obtained from Eq. (10).

To evaluate the result, we determined the correlation between the time series of the tendency error and the fit to the tendency error by the calculated linear com-

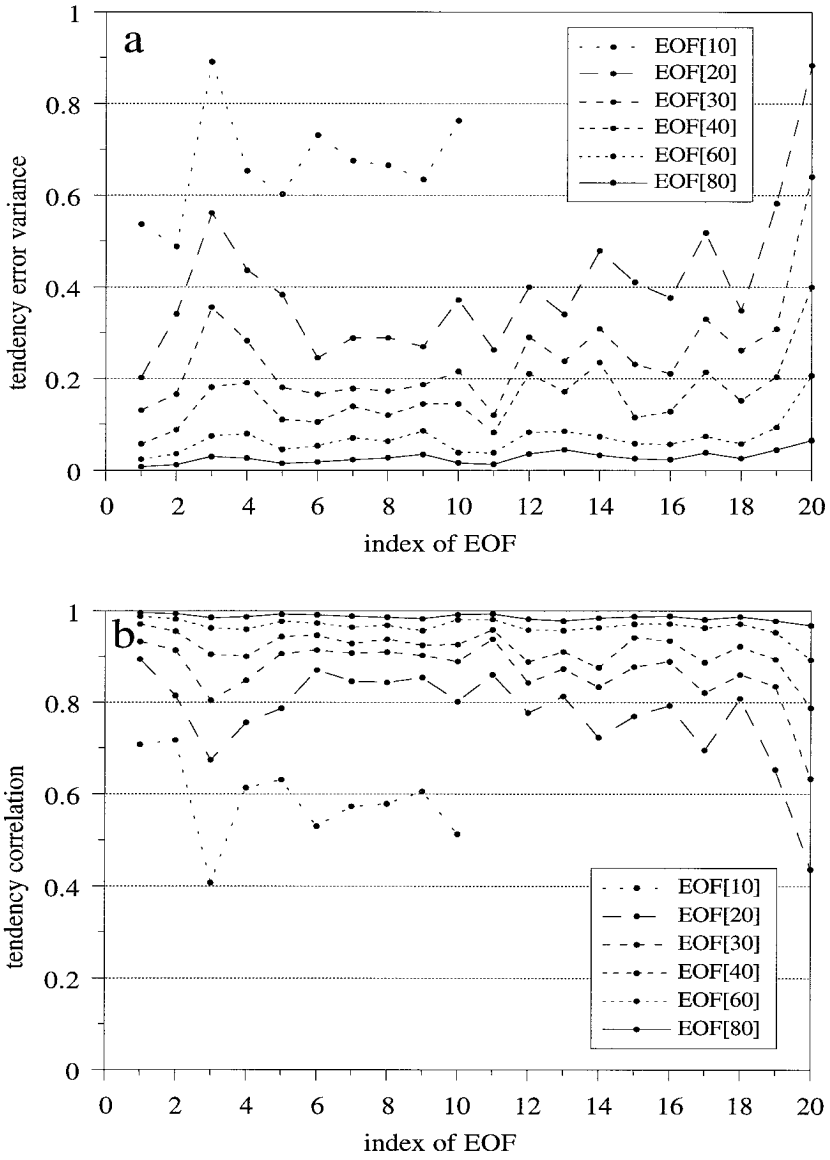

FIG. 1. (a) Variance of the tendency error of the first 20 EOFs for different truncations, divided by the variance of the true tendency. (b) Correlation between the true tendency and the tendency generated by the EOF model of the first 20 EOFs for various truncations.

bination of EOF amplitudes. These correlations are plotted in Fig. 2a for both sets of coefficients. The correlations are low. The two graphs (solid and dashed) are almost on top of each other, indicating that the sampling error in the estimated coefficients is small.

As an illustration, we plotted a 200-day time series of the tendency error of EOF 2 in Fig. 2b (dotted line), along with the linear fit deduced from each of the two 250 000-day datasets (solid and dashed lines). The amplitude of the linear fit remains close to zero, and its temporal behavior bears hardly any resemblance to the tendency error. The two fits are almost on top of each other, indicating that the sampling error in the estimated coefficients is small.

c. Quadratic corrections

Next we also adjusted the quadratic interaction terms in order to minimize the mean-squared tendency error at truncation 20. The bEOFs, the standard deviation of the bEOFs, the standard deviation of the tendency error, and the correlations between the bEOFs and the tendency error were estimated from both datasets of 250 000 days and substituted in Eq. (14) to obtain the corrections $\delta\beta_{ij}$ and $\delta\gamma_{ijk}$. The corrections to the constant terms $\delta\alpha_i$ were obtained from Eq. (10). Again we determined the correlation between the time series of the tendency error and the quadratic fit to the tendency error estimated from both datasets of 250 000 days. The cor-

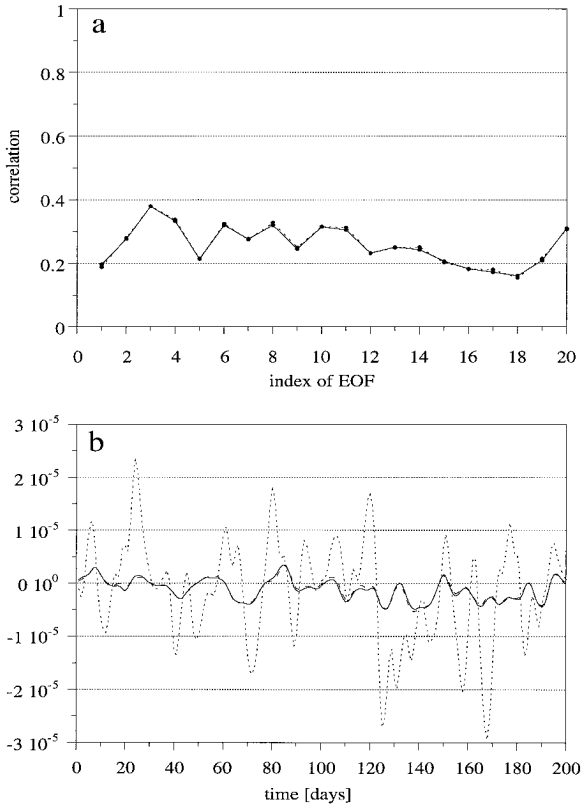

FIG. 2. (a) Correlation between the tendency error of the EOF model truncated to 20 EOFs and the approximation of the tendency error by a linear combination of EOF amplitudes. (b) Part of the time series from which the above correlation is calculated. The dotted line corresponds to the tendency error, and the solid and dashed lines to the approximation.

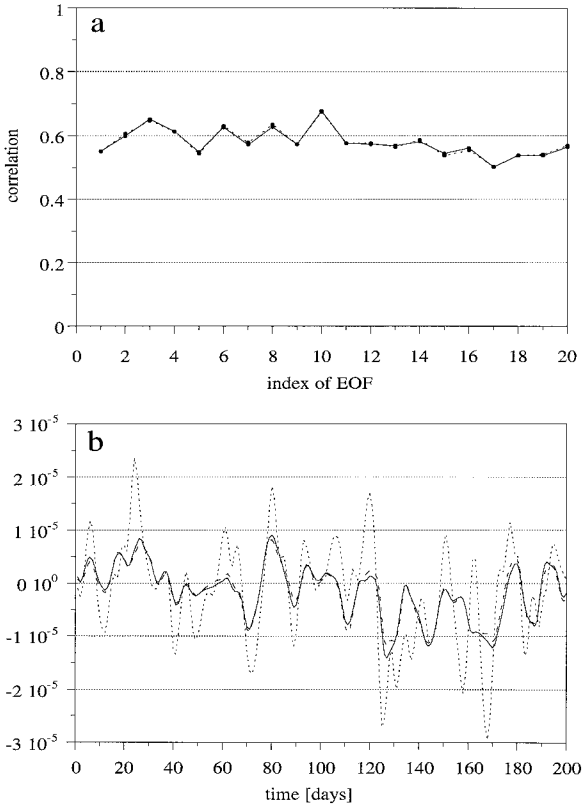

FIG. 3. (a) Correlation between the tendency error of the EOF model truncated to 20 EOFs and the approximation of the tendency error by a linear combination of EOF amplitudes and their quadratic combinations. (b) Part of the time series from which the above correlation is calculated. The dotted line corresponds to the tendency error, and the solid and dashed lines to the approximation.

relations are plotted in Fig. 3a. Compared with the results of the linear fit (Fig. 2a), the correlations are much higher. Again the sampling error appears small, as both fits show almost the same correlation. As an illustration, we plotted a 200-day time series of the tendency error of EOF 2 in Fig. 3b, along with both quadratic fits. Compared to the linear fit, the variations are much larger and bear more resemblance to the tendency error. With the adjusted EOF[20] model, we again calculated the tendency error variance and the correlation between the true tendencies and the tendencies of EOF[20]. The results are plotted in Fig. 4. The solid lines are the results for the closed EOF[20] model, the dotted lines for the model without closure. It is clear that the tendencies of the closed model are much closer to the true tendencies. Comparing the results with Fig. 1, it turns out that the closed EOF[20] model performs as well as EOF[30].

d. Prediction skill

In SE we used EOF[20] to predict the evolution of the circulation in the T21 model with 231 degrees of freedom. The forecasts started from states on the attractor of the T21 model, projected onto the first 20 EOFs. The EOF model was subsequently integrated for 3 weeks. At every day of the forecast, the predicted state EOF[20] was compared to the state of the T21 model by calculating anomaly correlation coefficients (ACC) between the streamfunction patterns and rms differences between the geopotential height fields. One hundred forecasts were performed with initial conditions selected from the 10 000-day dataset. The ACCs and rms values of these 100 forecasts were averaged to obtain a measure of the mean forecast skill of the EOF model. In this study, we repeated the same experiment with the adjusted EOF[20] model for both the linear and quadratic case. Note that the verification set is independent from the training set: the initial conditions are selected from the 10 000-day dataset, which is independent from the two 250 000-day datasets that were used to derive the optimal corrections that minimize the tendency error.

The results are plotted in Figs. 5a and 5b. Both graphs show that the mean prediction skill of EOF[20] is substantially improved by the closure including quadratic combinations of EOF amplitudes. Taking an ACC value

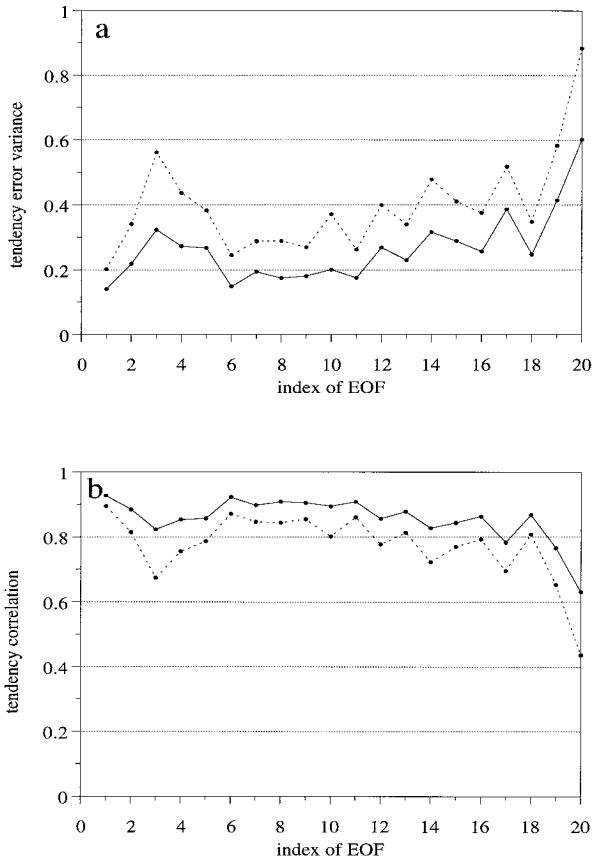

FIG. 4. As in Fig. 1 but for a truncation of 20 EOFs (dotted line). The solid line corresponds to the closed EOF model including quadratic combinations of EOF amplitudes.

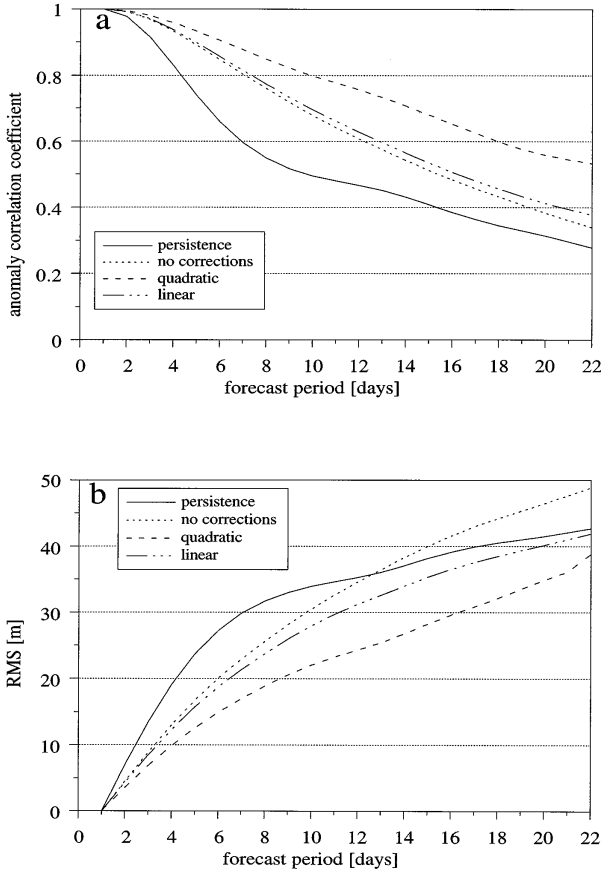

FIG. 5. (a) Average ACC of the streamfunction of 100 forecasts produced by various EOF[20] models and persistence (see legend). (b) As in (a) but for average rms errors of 500-hPa height.

of 0.6 as a lower boundary for a useful forecast, the mean range of a useful forecast has been increased by 6 days (from 12 to 18 days) due to the closure. The closure without the quadratic combinations of EOF amplitudes gives only a slight improvement in forecast skill (from 12 to 13 days). Clearly, for the purpose of a short-range forecast model, the proposed closure formulation including quadratic combinations of EOF amplitudes works quite well. It is interesting to note that although the closed EOF[20] model describes instantaneous tendencies as good as EOF[30], its forecast skill turns out to be much better. EOF[30] has an average useful forecast range of about 12 days (not shown) and, as said, the closed EOF[20] model 18 days.

e. Climate of the closed model

It is not clear a priori whether the closure also improves the long-term behavior of the low-order EOF model. The closure is determined from states on the attractor of the T21 model. Starting to integrate from a state on the attractor of the T21 model, the EOF model slowly turns away from the T21 model attractor. Although the closure improves the tendency of the EOF model on the attractor of the T21 model, it may introduce larger tendency errors in states off the attractor. This turned out to be the case when we tried to integrate the closed EOF[20] model (including corrections to the quadratic interaction coefficients) for an extended period in order to simulate the T21 model climate. At day 22 of the integration, the energy grew without bounds. It was verified that this catastrophe was not a numerical instability. Reducing the time step did not change the behavior. Apparently, the closed EOF[20] model does not possess a stable attractor. This is perhaps not so surprising since no restrictions are imposed on the applied corrections.

Let us take a closer look at the corrections. To evaluate the magnitude of the corrections with respect to the coefficients of the evolution equations, we determined the square root of the ratio between the sum of squares of the corrections and the sum of squares of the coefficients themselves. We did this for the constant terms, linear terms, and quadratic terms separately. The results are presented in Table 1 under column ''magnitude corrections'' in row ''all.'' It turns out that the corrections to the constant and linear coefficients are on average more than a factor of 10 larger than the coef-

TABLE 1. Results for different closures: constant (con), linear (lin), and quadratic (quad).

Coefficients	Magnitude corrections			$\bar{\rho}$	AUFR*	Crash
	Con	Lin	Qua			
All	14	20	1.3	0.6	18 d	22 d
100	12	12	0.6	0.5	16 d	70 d
50	11	6.5	0.26	0.4	15 d	500 d
25	5.7	3	0.08	0.3	13.5 d	—
Lin	1.8	0.8	—	0.22	13 d	—

* Average useful forecast range.

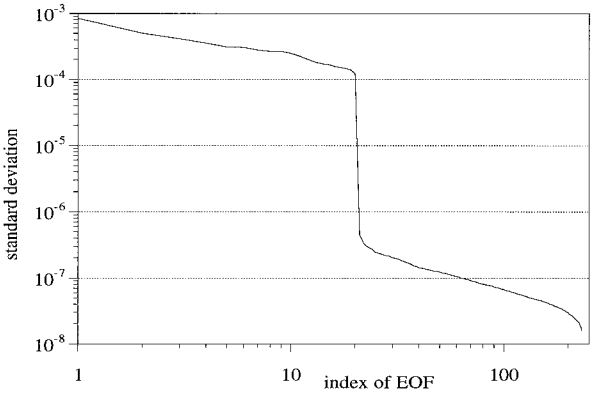

FIG. 6. Standard deviation of bEOFs determined from a 250 000-day dataset.

ficients themselves. The corrections to the quadratic terms are on average of about the same magnitude as the coefficients themselves. So we find large corrections that give relatively small tendency error reductions.

It might well be that the large corrections introduced by the bEOFs with small variances do not contribute that much to improving the fit to the tendency error, but do have a large impact on the instability that develops during a long-term integration. It might be, for instance, that the large corrections more or less cancel on the attractor but not off the attractor. This can be systematically investigated by removing the contributions of the bEOFs with small variances to the fit [exclude them in the sum in Eq. (14)] and then check the short- and long-term behavior of the closed model.

A plot of the standard deviations of the bEOFs is presented in Fig. 6. The first 20 bEOFs project mainly onto the EOF amplitudes. The remaining 210 bEOFs project mainly onto the quadratic combinations of EOF amplitudes and have much smaller standard deviations. We recalculated the corrections excluding bEOFs for which the ratio between the standard deviation of the tendency error and the standard deviaton of the bEOFs exceeds a certain value. Ratio values of 100, 50, and 25 were chosen. Since the standard deviation of the tendency error is not the same for every EOF, the number of bEOFs that still contribute to the regression (14) differs from EOF to EOF. At a ratio value of 100 (50, 25), on average about the first 95 (45, 25) of all 230 bEOFs are retained in the regression (14). With these different closures, we repeated the prediction experiments and the long-term integration.

The results are presented in Table 1 in rows 100, 50, and 25, respectively. The average magnitude of the corrections decreases as an increasing number of bEOFs with small standard deviations is excluded from the sum in Eq. (14). At the same time, however, the quality of the fit deteriorates (see column $\bar{\rho}$). The correlation between the tendency error and the fit to the tendency error averaged over all 20 EOFs decreases from 0.6 in case all bEOFs contribute to the fit down to 0.3 in case bEOFs are excluded for which the ratio between the standard deviation of the tendency error and their own standard deviation exceeds a value of 25. As a result, the average useful forecast range (AUFR) decreases from 18 days down to 13.5 days (see column ''AUFR''). On the other hand, the smaller corrections prevent unstable behavior for longer integration periods. For values of 100 and 50, the closed EOF model still explodes, but this happens at day 70 and day 500, respectively, compared to day 22 when all bEOFs contribute to the fit (see column ''crash''). For a value of 25 and in case only the linear and constant terms are adjusted (row ''lin''), the closed EOF[20] model possesses a stable attractor. However, in these cases the short-term prediction skill is hardly improved. It turns out that substantial corrections to the interaction coefficients are required to really improve the prediction skill, but this leads to unstable behavior.

To conclude this section, it is found that the proposed closure leads to a markedly improved prediction skill but at the same time unstable long-term behavior. We mention two modifications to the proposed closure that might solve this problem. One possibility is to impose restrictions on the allowed variations of the EOF model coefficients in order to ensure that the solution of the closed model stays bounded. One way to achieve this is to demand that in the closed model energy is conserved in the absence of forcing and dissipation. Another approach might be to determine the closure not from states on the attractor of the T21 model, but from states slightly off the attractor. In such states, the T21 model generates a tendency that is directed toward the attractor. If the closure is determined from these states, it will probably drive the closed EOF model toward the T21 model attractor.

4. Concluding remarks

In this paper, an attempt to close a low-order barotropic EOF model for the neglected interactions according to the proposition of Leith (1978) is described. We proposed to fit the tendency error of the model by a linear combination of known variables. In the case of the EOF model, we considered a linear combination of EOF amplitudes and quadratic combinations of these.

It was found that in order to obtain a reasonable description of the tendency error, the inclusion of quadratic combinations was required. Three-week forecasts made with the EOF model were improved considerably by this closure. However, the method seems questionable in two respects. First, the corrections to the coefficients of the evolution equations of the EOF amplitudes are as large as the coefficients themselves. Large corrections are found that give relatively small error reductions. For the closure to be meaningful, one would expect that to account for the small effect of the neglected interactions, it would suffice to slightly change the interactions between the resolved flow structures. Apparently this is not the case. The closure leads to a completely different model. It is therefore likely that the closure sensitively depends on the exact shape of the attractor and will lead to a completely different model for a slightly different attractor. Second, the closed EOF model could not simulate the climate. The model did not possess a stable attractor. As mentioned in the introduction, Faller and Schemm (1977) ran into the same problem in their attempt to close a simple two-dimensional advection model on a rectangular grid.

We mentioned two possible solutions to this problem. One possibility is to impose restrictions on the allowed variations of the EOF model coefficients in order to ensure that the solution stays bounded. One way to achieve this is to demand that energy is conserved in the absence of forcing and dissipation. Another approach might be to determine the closure not from states on the attractor of the T21 model, but from states slightly off the attractor. In such states, the T21 model generates a tendency that is directed toward the attractor. If the closure is determined from these states, it will probably drive the closed EOF model toward the T21 model attractor.

It remains to be seen whether the ability of the proposed closure to substantially improve the short-term prediction skill is not due to the simple form of the barotropic vorticity equation. Preliminary results in a two-layer quasigeostrophic model (U. Achatz 1995, personal communication) indicate that this is not the case.

As far as the applicability of the proposed closure to the practical problem of long-range forecasting is concerned, one must doubt that there is enough atmospheric data available to reliably fit the relatively large set of coefficients.

We conclude that the proposed closure without the mentioned modifications leads to a statistical model that gives better short-range predictions but fails to simulate the climate.

Acknowledgments. Many thanks are due to the predictability group at KNMI for a pleasant and stimulating atmosphere. I am grateful to Theo Opsteegh, head of this group, for his continuous support and help during this research.

REFERENCES

Achatz, U., G. Schmitz, and K. M. Greisiger, 1995: Principal interaction patterns in baroclinic wave cycles. *J. Atmos. Sci.,* **52,** 3201–3213.

Faller, A. J., and C. E. Schemm, 1977: Statistical corrections to numerical prediction equations. *Mon. Wea. Rev.,* **105,** 37–56.

Hasselman, K., 1988: PIPS and POPS: The reduction of complex dynamical systems using principal interaction and oscillation patterns. *J. Geophys. Res.,* **93** (D9), 11 015–11 021.

Illari, L., and J. C. Marshall, 1983: On the interpretation of eddy fluxes during a blocking period. *J. Atmos. Sci.,* **40,** 2232–2242.

Kwasniok, F., 1996: The reduction of complex dynamical systems using principal interactions patterns. *Physica D,* **92,** 28–60.

Leith, C. E., 1978: Objective methods for weather prediction. *Annu. Rev. Fluid Mech.,* **10,** 107–128.

Machenhauer, B., 1991: Spectral methods. *Proc. Numerical Methods in Atmospheric Models,* Reading, United Kingdom, European Centre for Medium-Range Weather Forecasts, 3–85.

MacVean, M. K., 1983: The effects of horizontal diffusion on baroclinic development in a spectral model. *Quart. J. Roy. Meteor. Soc.,* **109,** 771–783.

Press, W. H., B. P. Flannery, S. A. Teukolsky, and W. T. Vetterling, 1986: *Numerical Recipes—The Art of Scientific Computing.* Cambridge University Press, 818 pp.

Selten, F. M., 1993: Toward an optimal description of atmospheric flow. *J. Atmos. Sci.,* **50,** 861–877.

——, 1995: An efficient description of the dynamics of barotropic flow. *J. Atmos. Sci.,* **52,** 915–936.